Package Optimization of the Cilium-Type MEMS Bionic Vector Hydrophone

Liu Linxian, Zhang Wendong, Zhang Guojun, and Xue Chenyang

Abstract—We optimize the package of the cilium-type MEMS bionic vector hydrophone introduced by Chenyang and Wendong in 2007, which has the disadvantages of a low receiving sensitivity, narrow frequency band, and fluctuating frequency response curve. Initially, a full parametric analysis of frequency response and sensitivity with different material sound transparent cap were made. Then, we propose and realize an umbrella-type packaged structure with high receiving sensitivity and wide frequency band. The theoretical analysis and simulation analysis are conducted by ANSYS software and LMS virtual. Lab acoustic software. Finally, to verify the practicability of the package, the umbrella-type packaged hydrophone calibration was carried out in the National Defense Underwater Acoustics Calibration Laboratory of China. The test results show that the performance of umbrella-type hydrophone has been greatly improved compared with the previous packaged hydrophone: exhibiting a receiving sensitivity of −178 dB (increasing by 20 dB, 0-dB reference 1 V/μPa), the frequency response ranging from 20 Hz to 2 kHz (broaden one times), the fluctuation of frequency response curve within ±2 dB, and a good dipole directivity.

Index Terms—MEMS, umbrella-type packaged structure, receiving sensitivity, frequency response.

I. INTRODUCTION

THE vector hydrophone can not only detect the acoustic pressure signal and vibration velocity signal simultaneously, but also have dipole directivity. In the underwater acoustic measurement system, the use of the vector hydrophone improves the anti-interference ability and the line-spectrum detection ability [1]–[3]. Today, the study on vector hydrophones greatly attracts many research institutions. Leslie et al. fabricated a hydrophone to measure the water flow velocity by mounting a velocity pickup in a rigid, spherical Housing [4]. Fan Zhifang from University of Illinois at Urbana-Champaign reported the development of micromachined, distributed flow sensors based on a fish's lateral line [5]. N. Izadi1 from University at Bonn reported the fabrication of aquatic hair based flow sensors inspired by a

fish's lateral line [6]. Anders Heerfordt, et al developed a fiber hydrophone, which can work without electric power source, and is very applicable to the hydrophone towed array [7]–[8].

However, the development of acoustic technology and the weakness of the target signals have made high-sensitivity and low-frequency detection more and more urgent. Today, there are several critical problems about vector hydrophone to be solved: high-sensitivity, VLF (very low frequency) detection, miniaturization, anti-noise interference [9], [10].

To solve the above problems, Zhang Wendong, et al designed a kind of cilium-type MEMS bionic vector hydrophone by imitating the auditory principle of a fish's lateral line organ and using the bionic theory and piezoresistive principle [11], which has the advantages of miniaturization, rigid mounting, low-cost, good low-frequency characteristic, etc. The articles published previously focused on the process of the MEMS vector hydrophone and great achievements have been made [12], [13]. But there are still two key technology limitations in engineering application. Firstly, the receiving sensitivity of the hydrophone is low (−197.7 dB, 0 dB reference 1 V/μPa); secondly, the frequency band is narrow (20Hz∼ 800Hz).

In previous study [12], [13], we conclude that the package of the hydrophone is unreasonable. The resonance frequency of the sound transparent cap is too low and the cap's own various characteristics stack on the natural characteristic of the MEMS chip, resulting in a low receiving sensitivity, narrow frequency band and fluctuating frequency response curve. Therefore, this paper optimizes the packaged structure in several aspects, expecting to increase the resonance frequency of cap and to further improve the MEMS hydrophone performance. We study the influence of material of the sound transparent cap on frequency response and sensitivity, and then combining with acoustic wave equation, propose an "umbrella-type" packaged structure. Through the above improvement, the sensitivity has been increased by 20 dB and frequency band broaden by one times.

II. BIONIC PACKAGE PRINCIPLE

According to the bionic principle [14], [15], the sense-conducting pathway of a fish's lateral line organ can be obtained. Pressure in water will change under external force caused by sound waves, vibration waves and water flow velocity. This pressure travels into the lateral line canal through the lateral line pore, where the force is transferred to the mucus, causing the mucus to flow, which moves to the neuromast and
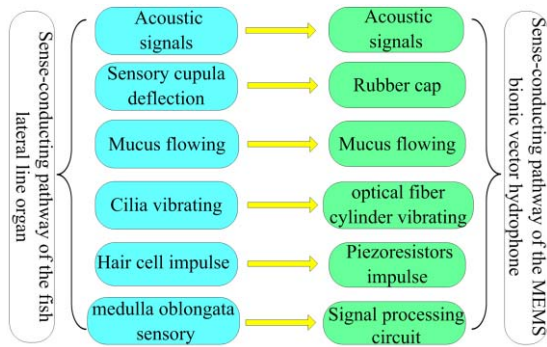
Fig. 1.   Bionic package principle of the vector hydrophone.

Fig. 2.   Package of the MEMS bionic vector hydrophone.

TABLE I
THE PROPERTIES PARAMETER OF SEAWATER AND SILICONE OIL

Material	seawater	silicone oil
Density ρ (kg/m^3)	1030	970
Poisson Ratio ν	-	-
Elastic modulus E (N/m^2)	-	-
Acoustic velocity c (m/s)	1570	1300
Characteristic impedance ρc (N·s/m³)	1.62×10^6	1.26×10^6

results in motion of the sensory cupula. The motion of the cupula results in deflection of the kinocilia via the lymphatic mucus flowing into the cupula. The kinocilia is the relevant mechanical stimulus for the hair cells. Thus, the hair cells are stimulated, then the signals are transferred to the medulla oblongata through the sensory nerve fibers and the lateralis nerve [16]–[18].

When applied in underwater detection, the microstructure of MEMS vector hydrophone cannot detect underwater signals directly without a sound-transparent, insulated and waterproof package. A shell should be designed to isolate hydrophone microstructure from water. Additionally, to improve the anti-pressure ability of the entire structure and avoid bubbles, the shell must be filled with liquids. Furthermore, the material of the shell must have good sound-transparent characteristic to ensure that acoustic signals can be maximally transferred to cilium.

To this end, according to the sense-conducting pathway of a fish's lateral line organ, the bionic package principle of the cilium-type MEMS bionic vector hydrophone [11]–[13] is shown in Fig. 1. In packaging, the cap (shell) is made of sound-transparent polyurethane, and the insulating silicone oil has a low viscosity with a characteristic impedance very near that of water, is poured into the cap. As shown in Fig. 2, the cupula, mucus, kinocilia, hair cells and nerve fibers are replaced by rubber cap, silicone oil, optical fiber cylinder, piezoresistors and wire, respectively. When an underwater acoustic signal is applied on the rubber cap (cupula), the silicone oil (mucus) will transmit the signal to the optical fiber cylinder (cilia). The movement of the optical fiber cylinder causes deformation of the beams. Consequently, the resistance of the silicon piezoresistors (hair cells) on the beams will change. When there is incentive direct current, the change in the resistances will be converted to an output voltage using a Wheatstone bridge via the metal wire (efferent lateralis neuron). Therefore, the underwater spatial acoustic signal will be detected.

III. IMPROVEMENT OF PACKAGE

Two key issues should be considered while designing the acoustic packaged structure of the cilium-type MEMS bionic vector hydrophone: broaden frequency band and increase sensitivity. On the basis of previous work [11]–[13], we know
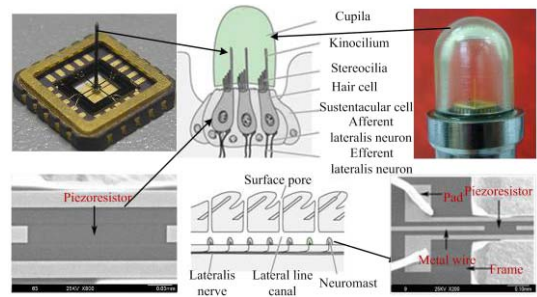
that the mainly results leading to the narrow frequency band is the resonance frequency of the sound transparent cap is too low. So, firstly, a full parametric analysis of frequency response and sensitivity with different material sound transparent cap were made. Then, we propose an "umbrella"-type packaged structure.

A. Effects of the Sound Transparent Cap Material Properties on Frequency Response and Sensitivity

In order to explore the effects of the different material properties, we compared the resonance frequency of the sound-transparent cap and sound-transmission coefficient of the cap by changing Young's modulus E, Poisson's ratio ν and the density ρ.

The coupled modal and the acoustic attenuation of the sound-transparent cap with different material properties are simulated by LMS virtual. Lab acoustic [19]. Sound fields are established, as shown in Fig. 8(a). The radius and height of the sound-transparent cap are determined on the basis of the four-beam microstructure: height is 20 mm, radius is 12.5 mm, and thickness is 2 mm, respectively.

The process of simulation is as follows: firstly, finite element 3D model is created by ANSYS including the sound-transparent cap, silicone oil inside the cap and seawater outside the cap; then import it into LMS virtual. Lab acoustic; after which, define A field point (in silicone oil inside the cap) and B field point (in seawater outside the cap), as shown in Fig. 8(a), and define the acoustic resource intensity as 1Pa. The properties parameter of seawater and silicone oil used are given in Table I.

Fig. 3 shows the deformation diagram of the seawater-cap-silicone oil coupled modal. First, we obtained the resonance frequency from the coupled modal analysis, as shown in Fig. 4. Fig. 4(a) shows that the resonance
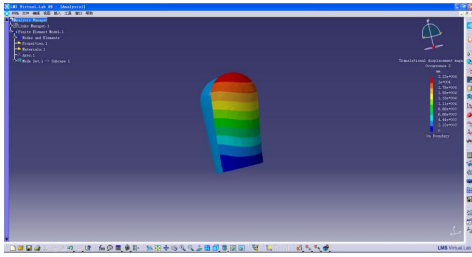
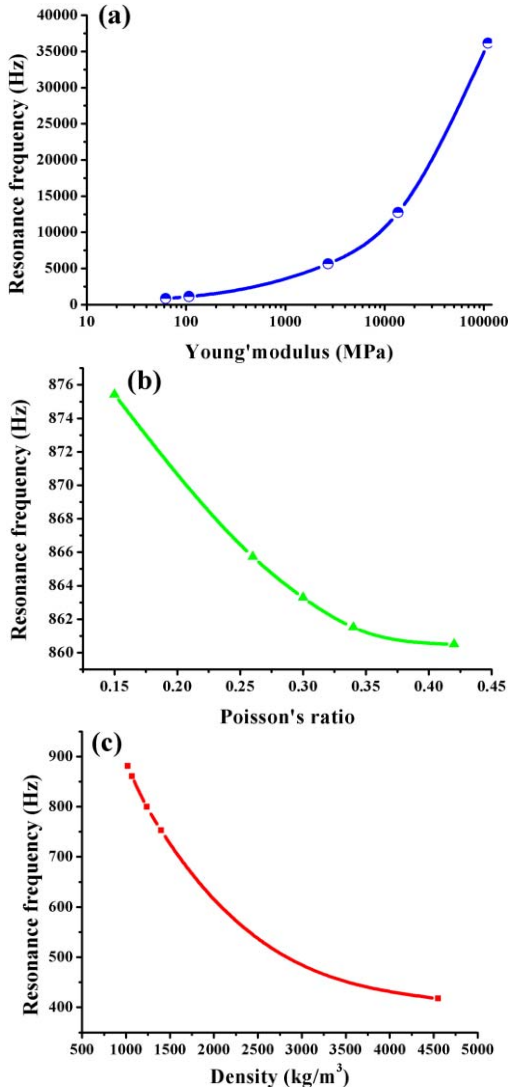Fig. 3. Deformation diagram of the seawater-cap-silicone oil coupled modal.

Fig. 4. Resonance frequency, by varying (a) the Young's modulus E (for $\rho = 1070$kg/m3, $\nu = 0.42$), (b) the Poisson's ratio ν (for $E = 62.5$MPa, $\rho = 1070$kg/m3), and (c) the density ρ (for $E = 62.5$MPa. $\nu = 0.42$).

frequencies increase with the increasing of the Young's modulus E, for fixed density $\rho = 1070$kg/m3 and Poisson ratio $\nu = 0.42$. Fig. 4(b) and (c) shows that the resonance frequencies decrease with the increasing of the Poisson's ratio (for $E = 62.5$MPa, $\rho = 1070$kg/m3) and the density (for $E = 62.5$MPa, $\nu = 0.42$).

The sound-transmission coefficient τ can be expressed as the ratio between the transmission sound intensity level I_t and
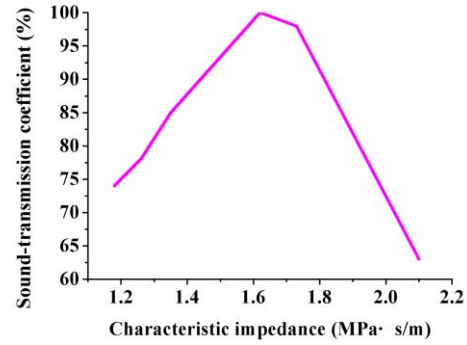

Fig. 5. The sound-transparent coefficient for various characteristic impedance of materials (at 1 kHz).

the incidence sound intensity level I_i [20]

$$\tau = \frac{I_t}{I_i} = (\frac{p_t}{p_i})^2 \tag{1}$$

where p_t, p_i are the transmission acoustic pressure and incidence acoustic pressure, respectively.

We extract the sound at point A (inside the cap) and point B (outside the cap) respectively with different characteristic impedance. And the sound-transmission coefficient can be calculated according to equation (1). Fig. 5 illustrates the effects of the changing of characteristic impedance on the sound-transmission coefficient at 1 kHz. It can be concluded that, in order to obtain the highest the sound-transparent coefficient, the characteristic impedance of materials should be equal to or close to that of seawater.

Then, we consider four basic materials for the sound-transparent cap, which are particularly suited to underwater applications in view of their adhesion and waterproof. And the elastic properties are given in Table II.

The first four coupled modes for the four different materials cap are shown in Fig. 6. And the sound-transparent coefficient for the four different materials cap are shown in Fig. 7 (the simulation frequency is 50Hz $\sim$ 2500Hz).

Figs. 6 and 7 show that although the resonance frequencies of the nylon1010, polysulfone and FRP sound-transparent cap are 4.17 KHz, 6.19 KHz and 13.5 KHz respectively, which are far higher than that of polychloroprene sound-transparent cap (0.875 KHz); the sound transmission performance clearly deteriorates, which decreases the sensitivity of hydrophone to a great extent.

The objective of designing the packaged structure is to broaden frequency band of the hydrophone and to improve frequency response without decreasing the sensitivity. So, although the nylon1010, polysulfone and FRP caps can realize the improvement of frequency respond and broadness of the frequency band, the sensitivity is decreased too much. Therefore, in view of the above analysis, the method by using other materials to replace polyurethane cap is impractical. It could be reasonable to ascertain that there is no material able to improve the performance of the hydrophone.

B. "Umbrella"-Type Packaged Structure

According to section A, we know that the method by changing the materials of sound-transparent cap is impractical.

TABLE II
THE PROPERTIES PARAMETER OF DIFFERENT MATERIALS

Material	polychloroprene	nylon1010	polysulfone	FRP
Density $\rho\,(kg/m^3)$	1070	1023	1240	1400
Poisson Ratio ν	0.42	0.3	0.26	0.15
Elastic modulus $E\,(N/m^2)$	6.25e7	1.07e9	2.69e9	1.37e10
Acoustic velocity c（m/s）	1620	1150	1100	1500
Characteristic impedance ρc (N·s/m³)	1.73 e6	1.18 e6	1.35 e6	2.10 e6
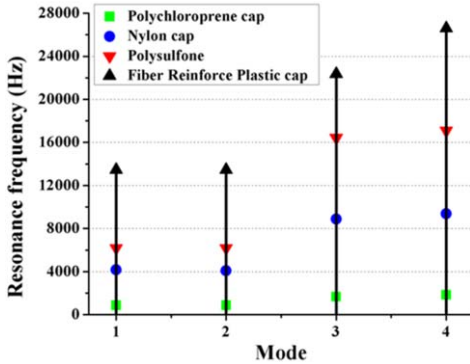
Fig. 6. The first four coupled modes for the four different materials.

Fig. 8. Pre-packaged structure (a) and "umbrella-type" packaged structure (b) for the hydrophone.
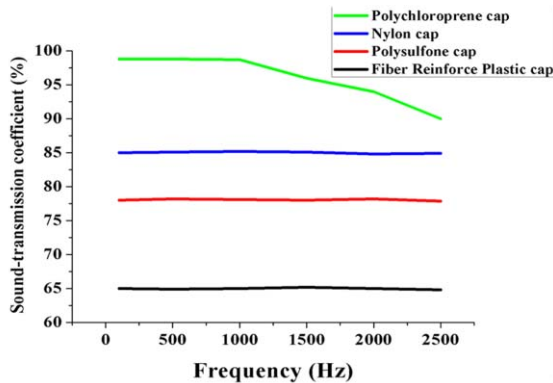

Fig. 7. The sound-transparent coefficient for the four different materials.

Fig. 9. 3D model of "umbrella-type" packaged structure.

Among the acoustic–electric transducer structure, the optical fiber cylinder plays the role of detecting the acoustic waves and can directly sense the acoustic particle motion. So we propose an "umbrella-type" packaged structure combining with the acoustic continuity equation, as shown in Fig. 8(b). The "umbrella-type" packaged structure can centralize acoustic power on the optical fiber cylinder, which improves the acoustic receiving efficiency as well as the sensitivity of the hydrophone. Meanwhile, the rigid support frame is adhered to the inner side of the cap, which makes sound-transparent cap structure more rigid as well as broadens the frequency band of the hydrophone. The parameters of the "umbrella-type" rigid support frame are determined based on the structure of sound transmission-cap. A three-dimensional model of the "umbrella-type" packaged structure is shown in Fig. 9.
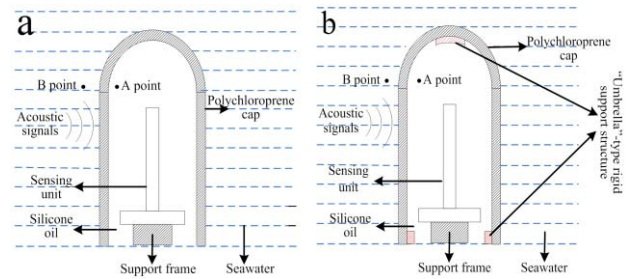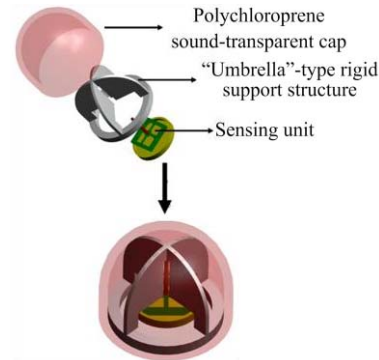
Theoretical analysis, simulations and experiments are carried out to verify the practicability of the "umbrella-type" packaged structure.

1) The Theoretical Analysis of the Effects of the "Umbrella-Type" Packaged Structure on Sensitivity and Frequency Response: Fig. 10. shows the schematic diagram of sound propagation with "umbrella-type" packaged structure. Continuous medium can be seen as a material system which is composed of many inextricably linked volume element. The medium in the volume element can be treated as a particle. Take a volume element "dV" of silicone oil in the "umbrella-type" packaged structure, as shown in Fig. 11.

From Fig. 10, we can see that the sectional area of the silicone oil in the "umbrella-type" packaged structure is gradually shrinkage. So according to the mass conservation law and fluid continuity equation, the mass variations in the volume element closer to the optical fiber cylinder is more than that in the
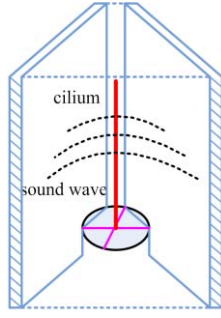
Fig. 10. Schematic diagram of acoustic propagation in "umbrella-type" packaged structure.

Fig. 12. The first sixth resonance frequency of pre-packaged structure and "umbrella-type" packaged structure.
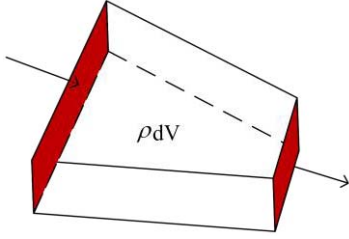

Fig. 11. The volume element model of silicone oil in the "umbrella-type" packaged structure.

volume element away from the optical fiber cylinder, that is

$$\rho_1 dV > \rho_2 dV \tag{2}$$

where, ρ_1 and ρ_2 are the average density variations in the volume element closer to the optical fiber cylinder and away from the optical fiber cylinder in presence of a small-amplitude acoustic wave.

So,

$$\rho_1 > \rho_2 \tag{3}$$

Acoustic waves in an ideal fluid are adiabatic, so that the pressure P and density ρ' small perturbations are related by the equation of state [20], [21]

$$p = c_0^2 \rho' \tag{4}$$

with c_0 denoting the speed of sound in the fluid.

Therefore, the acoustic pressure P_1 in the volume element closer to the optical fiber cylinder is greater than the acoustic pressure P_2 in the volume element away from the optical fiber cylinder

$$p_1 > p_2. \tag{5}$$

Acoustic energy in volume element is [21]:

$$\Delta AE = \frac{dV}{2} \rho_0 \left(v^2 + \frac{1}{\rho_0^2 c_0^2} p^2 \right) \tag{6}$$

where, ρ_0 is the medium density without acoustic perturbation, P is the acoustic pressure with acoustic perturbation, v is the medium particle velocity.

So, we can conclude that the acoustic energy ΔAE_1 in the volume element closer to the optical fiber cylinder is greater
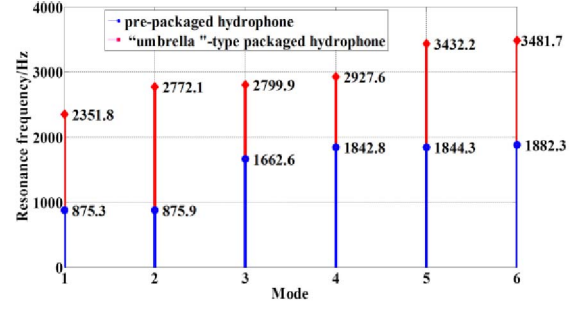
than the acoustic energy ΔAE_2 in the volume element away from the optical fiber cylinder.

$$\Delta AE_1 > \Delta AE_2 \tag{7}$$

Therefore, the "umbrella-type" packaged structure can gather energy, and increase the sensitivity of hydrophone.

Moreover, to ensure that the mechanical properties of the packaged structure cannot affect the sensitivity and frequency response, the first resonance frequency of the sound-transparent cap must be far higher than that of MEMS chip (sensing units). In the previous packaged structure, the first resonance frequency of the cap is lower than that of MEMS chip [11]–[13], which severely affects the performance of the hydrophone. Compared with the previous package, the "umbrella-type" packaged structure adds a metal rigid support frame adhered to the inner side of the cap, which makes sound-transparent cap structure more rigid as well as improves the elasticity coefficient. Theoretically, it approximately equivalent to the situation that a closed box is divided into 4 equal parts, and each mass is

$$M_1 = M_2 = M_3 = M_4 = \frac{1}{4} M \tag{8}$$

where M_1, M_2, M_3, M_4 are the distinguished-mass, M is the total mass.

The resonance frequency of the structure is

$$F = \frac{1}{2\pi} \sqrt{\frac{K}{m}} \tag{9}$$

According to the equation (9), we can conclude that the resonance frequency of the "umbrella"-type packaged structure approximately is 2 times higher than that of the pre-packaged structure.

2) The Simulated Analysis of the Effects of the "Umbrella-Type" Packaged Structure on Sensitivity and Frequency Response: To verify the validity of the theoretical analysis, we carried out the acoustic simulation by ANSYS and LMS virtual. Lab acoustic.

a) Modal analysis and Harmonic response analysis: The modal analysis and harmonic response analysis are conducted, and the first sixth resonance frequency of pre-packaged structure and "umbrella"-type package structure are shown in Fig. 12. Figs. 13 and 14 show the first mode of pre-packaged structure and "umbrella-type" packaged structure. Fig. 15 shows the harmonic response of "umbrella"-type
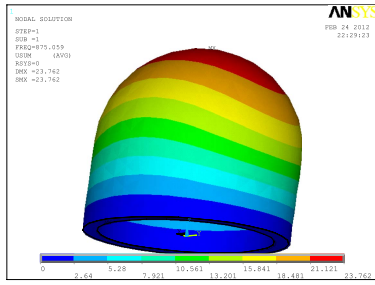
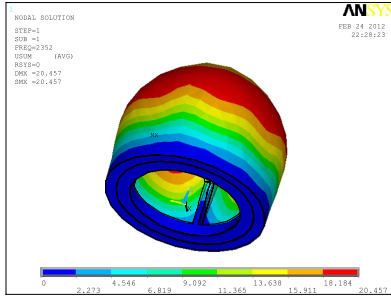Fig. 13.   The first mode of pre-packaged structure.

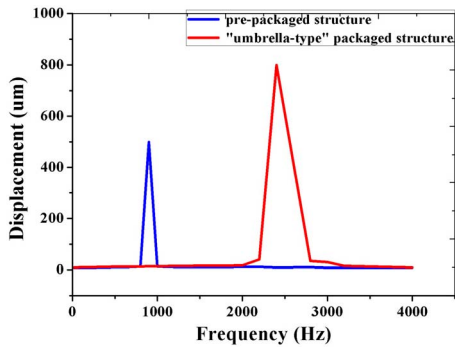Fig. 14.   The first mode of "umbrella-type" packaged structure.

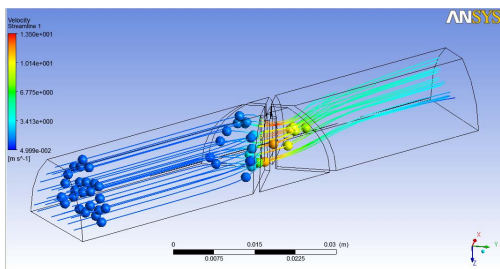Fig. 15.   Harmonic response of pre-packaged structure and "umbrella-type" packaged structure.

Fig. 16.   The cohesive energy model of "umbrella-type" packaged structure.

package structure. It can be seen that the first resonance frequency of the "umbrella"-type packaged structure is nearly 2∼3 times higher than the pre-packaged structure, as well as far higher than that of MEMS chip. The simulation results keep consistent with the theoretical analysis results.

b) Acoustic analysis: Fig. 16 illustrates the cohesive energy model of "umbrella-type" packaged structure by
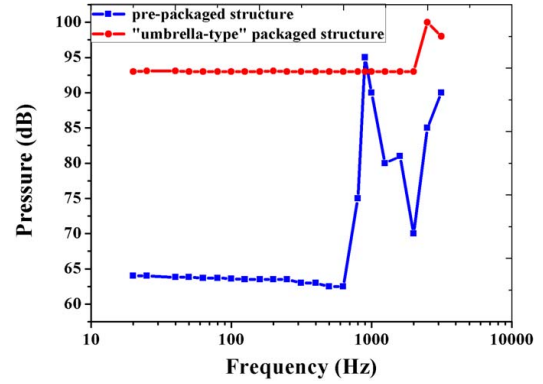

Fig. 17.   Acoustic pressure curve inside the cap of pre-packaged structure and "umbrella-type" packaged structure.
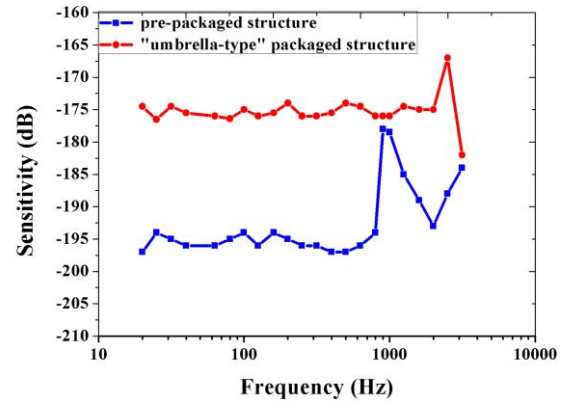

Fig. 18.   Simulated sensitivity of pre-packaged structure and "umbrella-type" packaged structure.

ANSYS. It can be seen that the particle velocity is obviously much larger at the location closer to the optical fiber cylinder than that of the locations away from the optical fiber cylinder, which is agreement with the theoretical analysis.

We extract the acoustic pressure at point A (inside the cap) with pre-packaged structure and "umbrella-type" packaged structure respectively in LMS virtual. Lab acoustic. Fig. 17 shows the acoustic pressure inside the cap, respectively, as a function of frequency. It can be seen that the acoustic pressure inside the cap with "umbrella-type" packaged structure is higher than that with pre-packaged structure.

The sensitivity can be expressed as by the voltage output at a unit sound pressure (1Pa), for the P-type piezoresistors:

$$S_V = \frac{V_{out}}{P_u} = \frac{\Delta R}{R} \times V_{in} = 71.8 \times \sigma_1 \times 10^{-11} \times V_{in} \quad (10)$$

where σ_1 is the longitudinal stress, V_{in} is the input voltage. We can obtain the simulated stress on the location of the piezoresistors under different acoustic pressure by static analysis, and then the sensitivity in presence of an acoustic wave at different frequencies can be calculated according to equation (8). Fig. 18 shows the calculated pressure sensitivity (0 dB reference 1 V/uPa). It can be seen that the simulated sensitivity of the "umbrella"-type packaged hydrophone is up to −175dB, which increases nearly by 20 dB comparing with the pre-packaged hydrophone (−195.5 dB).
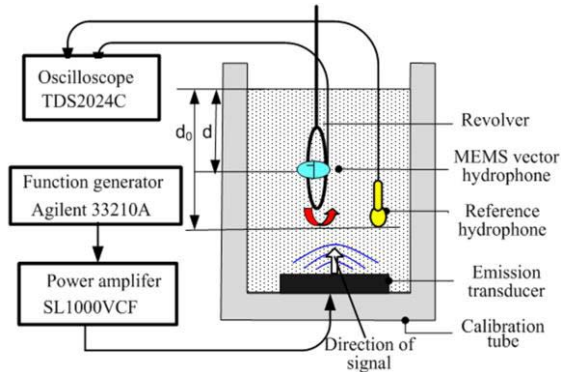
Fig. 19. Photograph of the packaged hydrophone.

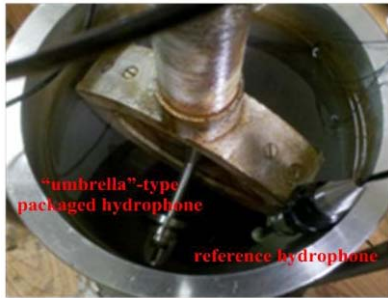Fig. 20. Schematic of the measurement system.

Fig. 21. Photograph of the measurement system.

IV. CALIBRATION TEST

The packaged vector hydrophone is shown in Fig. 19. To verify the performance of the "umbrella-type" hydrophone, the Calibration of the hydrophone was processed in a standing wave field in the National Defense Underwater Acoustics Calibration Laboratory of China. The measurement system includes a function generator, a power amplifier, a calibration tube, data acquisition system, and revolver. Schematic diagram of the test setup is shown in Fig. 20. The reference hydrophone was hung in water and the tested hydrophone was fixed on the revolver, as shown in Fig. 21.

The sensitivity test adopts a standing wave comparison calibration, i.e., the open-circuit voltage output of the tested MEMS hydrophone is compared with the reference hydrophone to determine the sensitivity of the tested
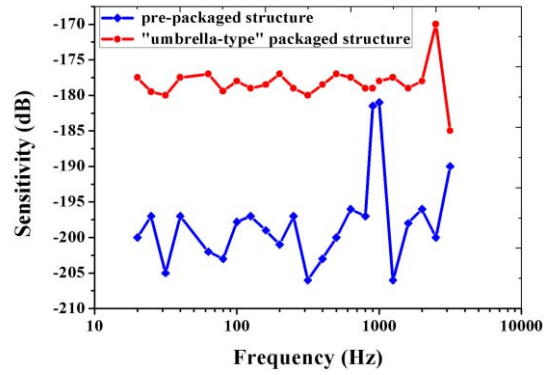

Fig. 22. Frequency response of pre-packaged and "umbrella-type" packaged MEMS Bionic Vector Hydrophone.
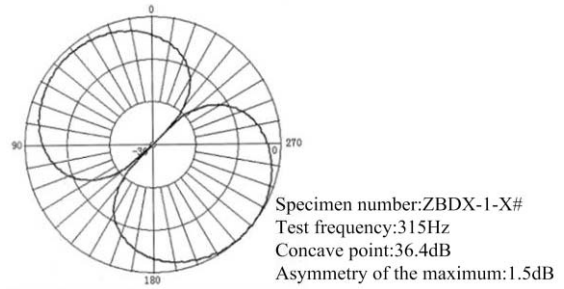

Fig. 23. Directivity pattern of "umbrella-type" packaged MEMS Bionic Vector Hydrophone at 315 Hz.

hydrophone. Fig. 22 depicts the frequency response of the pre-packaged hydrophone and "umbrella"-type packaged hydrophone. It can be seen that the receiving sensitivity of the "umbrella"-type packaged hydrophone reaches −178 dB (0 dB reference $1V/\mu Pa$), increased by 20 dB comparing with the pre-packaged hydrophone, and that the frequency band ranges from 20 Hz to 2 KHz (broaden one times).More importantly, the fluctuation of the curve is within ±2dB (decreased by ±3 dB). The directivity pattern of the "umbrella"-type packaged hydrophone at the frequency of 315 Hz are depicted in Fig. 23, which shows that the hydrophone has a good directional pattern in the form of an "8" shape(dipole directivity) and good symmetry, where the concave point depth reaches 38.4 dB.

V. CONCLUSION

We studied the influence of material of the sound transparent cap on frequency response and sensitivity of the cilium-type MEMS bionic vector hydrophone introduced by Zhang Wendong, etc. In connection with the sound-transparent cap elastic properties, high value of the Young's modulus, low values of Poisson's ratio and density are desirable for enhancing the resonance frequency, and in order to obtain the highest the sound-transparent coefficient, the characteristic impedance of cap materials should be equal to or close to that of seawater. Four basic materials particularly suited to underwater applications were considered. Our full numerical analysis results indicate that by using other materials to replace polyurethane cap is impractical.

So, based on the fluid continuity equation, an "umbrella"-type packaged structure of the hydrophone is proposed, which can improve the sensitivity by gathering energy and broaden the frequency band by increasing the resonance frequency of the sound-transparent cap structure. The test results verify the effectiveness of the "umbrella-type" packaged structure. Compared with the pre-packaged structure, the receiving sensitivity of hydrophone is increased by 20 dB and the frequency band is broadened by one times. Additionally, the fluctuation of frequency response curve is decreased by 3 dB. The hydrophone exhibits a good directional pattern in the form of an "8"-shape, and the curve is smooth. The experimental results keep agreement with the theoretical analysis and simulations, confirming the correct modeling of the hydrophone as well as its prediction capability, further verifying the feasibility of detecting underwater acoustic signals by the "umbrella-type" packaged hydrophone, which establish foundation for further engineering application.

REFERENCES

[1] J. A. McConnel, "Analysis of a compliantly suspended acoustic velocity sensor," *J. Acoust. Soc. Amer.*, vol. 113, no. 3, pp. 1395–1405, 2003.

[2] B. M. Abraham, "Low-cost dipole hydrophone for use in towed arrays," in *Proc. AIP Conf.*, vol. 368. Sep. 1995, pp. 189–201.

[3] A. Nehorai and E. Paldi, "Vector-sensor array processing for electromagnetic source localization," *IEEE Trans. Signal Process.*, vol. 42, no. 2, pp. 376–398, Feb. 1994.

[4] C. B. Leslie, J. M. Kendall, and J. L. Jones, "Hydrophone for measuring particle velocity," *J. Acoust. Soc. Amer.*, vol. 28, no. 4, pp. 711–715, 1956.

[5] Z. F. Fan, J. Chen, J. Zou, D. Bullen, C. Liu, and F. Delcomyn, "Design and fabrication of artificial lateral line flow sensors," *J. Micromech. Microeng.*, vol. 12, no. 5, pp. 655–661, Sep. 2002.

[6] N. Izadi and M. J. de Boer, "Fabrication of dense low sensor arrays on flexible membranes," in *Proc. Int. Solid-State Sensors, Actuat. Microsyst. Conf.*, Jun. 2009, pp. 1075–1078.

[7] A. Heerfordt, B. Møhl, and M. Wahlberg, "A wideband connection to sperm whales: A fiber-optic, deep-sea hydrophone array," *Deep Sea Res. I, Oceanograph. Res. Papers*, vol. 54, no. 3, pp. 428–436, Mar. 2007.

[8] P. E. Bagnoli, N. Beverini, R. Falciai, E. Maccioni, M. Morganti, F. Sorrentino, *et al.*, "Development of an erbium-doped fibre laser as a deep-sea hydrophone," *J. Opt. A, Pure Appl. Opt.*, vol. 8, no. 7, pp. 535–539, 2006.

[9] T. B. Gabrielson and D. L. Gardner, "A simple neutrally buoyant sensor for direct measurement of particle velocity and intensity in water," *J. Acoust. Soc. Amer.*, vol. 97, no. 4, pp. 2227–2237, 1995.

[10] P. Palanisamy, N. Kalyanasundaram, and P. M. Swetha, "Two-dimensional DOA estimation of coherent signals using acoustic vector sensor array," *Signal Process.*, vol. 92, no. 1, pp. 19–28, Jan. 2012.

[11] C. Y. Xue, S. Chen, and W. D. Zhang, "Design, fabrication, and preliminary characterization of a novel MEMS bionic vector hydrophone," *Microelectron. J.*, vol. 38, nos. 10–11, pp. 1021–1026, Nov. 2007.

[12] C. Y. Xue, Z. M. Tong, B. Z. Zhang, and W. D. Zhang, "A novel vector hydrophone based on the piezoresistive effect of resonant tunneling diode," *IEEE Sensors J.*, vol. 8, no. 4, pp. 401–402, Apr. 2008.

[13] W. D. Zhang, L. G. Guan, and G. J. Zhang, "Research of DOA estimation based on single MEMS vector hydrophone," *Sensors*, vol. 9, no. 9, pp. 6823–6834, Aug. 2009

[14] H. M. Muller, "Indications for feature detection with the lateral line organ in fish," *Comparat. Biochem. Physiol. A, Physiol.*, vol. 114, no. 3, pp. 257–263, Jul. 1996.

[15] S. S. Jande, "Fine structure of lateral-line organs of frog tadpoles," *J. Ultrastruct. Res.*, vol. 15, no. 5, pp. 496–509, Aug. 1966.

[16] W. K. Metcalfe, C. B. Kimmel, and E. Schabtach, "Anatomy of the posterior lateral line system in young larvae of the zebrafish," *J. Comparat. Neurol.*, vol. 233, no. 3, pp. 377–389, Mar. 1985.

[17] S. Dijkgraaf, "The functioning and significance of the lateral-line organs," *Biol. Rev.*, vol. 38, no. 1, pp. 51–105, 1963.

[18] O. Sand, "The lateral line and sound reception," in *Hearing and Sound Communication in Fishes*, W. N. Tavolga, A. N. Popper, and R. R. Fay, Eds. New York, NY, USA: Springer-Verlag, 1981, pp. 459–480.

[19] Z. G. Li and F. L. Zhan, *Acoustic Simulation Calculation Application*. Beijing, China: National Defense Industry Press, 2010, pp. 112–157.

[20] L. D. Landau and E. M. Lifshitz, *Fluid Mechanics*. New York, NY, USA: Pergamon, 1987.

[21] G. H. Du and Z. M. Zhu, *Acoustic Foundation*. Nanjing, China: Nanjing Univ. Press, 2010.

Liu Linxian was born in Shanxi, China, in 1987. She received the master's degree in precision instrument and mechanism from the North University of China, Shanxi, in 2013, where she is currently pursuing the Doctoral degree in precision instrument and mechanism. Her research interests include N/MEMS devices and hydrophone's designing and optimization.

Zhang Wendong is the President of the Taiyuan University of Technology. He was born in Henan, China, in 1962. He received the Doctoral degree from the Beijing Institute of Technology in 1995. In 1996, he was with Tsinghua University as a Post-Doctoral Fellow. He engages in researching and teaching in measurement technology and micro/nanotechnology field. Two second-class of national invention medals, one third-class of national invention medals. He has received 13 items of State Science and Technology Advancement Prize, he holds ten items of invention patent, and he has published 190 academic papers, three printed monographs, and one translated book.

Zhang Guojun was born in Shandong, China, in 1977. He received the master's degree in acoustics technology from the Institute of Acoustics, Chinese Academy of Sciences, in 2006. He engages in researching and teaching in MEMS sensor, acoustics, semiconductor physics, and has published ten academic papers in MEMS hydrophone, four of which has been embodied by SCI, seven has been embodied by EI.

Xue Chenyang was born in Shanxi, China, in 1971. He received the Doctoral degree from the National Technical University of Athens in 2003. He is currently a Post-Doctoral Fellow with the North University of China. He engages in researching and teaching in micro-nanosensor technology and its application. He has published more than 40 articles in microelectronic engineering, sensors and actuators, and international conferences, of which more than 20 by SCI and EI.